FERMILAB-CONF-16-501-CMS-E
ACCEPTED

Prepared for submission to JINST

Topical Workshop on Electronics for Particle Physics 2016,
September 26-30, 2016
Karlsruhe, Germany

The upgrade of the CMS hadron calorimeter with silicon photomultipliers

N. Strobbe on behalf of the CMS collaboration

Fermi National Accelerator Laboratory,
Batavia, Illinois, U.S.A.

E-mail: nstrobbe@fnal.gov

Abstract: The upgrade of the hadron calorimeter of the CMS experiment at the CERN Large Hadron Collider is currently underway. The endcap sections will be upgraded in the winter of 2016–2017 and the barrel sections during the second LHC long shutdown in 2019. The existing photosensors will be replaced with about 16 000 new silicon photomultipliers (SiPMs), resulting in the first large installation of SiPMs in a radiation environment. All associated front-end electronics will also be upgraded. This paper discusses the motivation for the upgrade and provides a description of the new system, including the SiPMs with associated control electronics and the front-end readout cards.

Keywords: Calorimeters; Front-end electronics for detector readout; Radiation-hard electronics

This document was prepared by CMS collaboration using the resources of the Fermi National Accelerator Laboratory (Fermilab), a U.S. Department of Energy, Office of Science, HEP User Facility. Fermilab is managed by Fermi Research Alliance, LLC (FRA), acting under Contract No. DE-AC02-07CH11359

Contents

1 Introduction

The CMS hadron calorimeter (HCAL) [1] consists of 17 layers of brass absorber and scintillator tiles in barrel (HB) and endcap (HE) sections, complemented by an outer (HO) and quartz-fiber forward (HF) detector. The focus of this paper is on the HB and HE detectors, more details on HO and HF can be found in refs. [2, 3]. In the current CMS detector wavelength-shifting fibers transport the scintillation light from the HB and HE tiles to hybrid photodiodes (HPDs) [4], whose electric signals are then integrated and digitized by the Charge Integration and Encoder version 8 (QIE8) ASIC [5, 6] before being sent to off-detector readout electronics.

The CMS HCAL detector has been operating successfully throughout Run 1 and the ongoing Run 2 of the CERN Large Hadron Collider (LHC). However, radiation damage has caused the scintillator tiles to darken. Given the expected integrated luminosity of 3–5 ab^{-1} to be delivered by the LHC over the next 15–20 years, corresponding to 10^{12} neutrons/cm^2, 10 krad of ionizing dose, and 10^{11} 20 MeV hadrons/cm^2, it is clear that mitigation strategies need to be put in place in order to retain the ability to reconstruct signals of particles showering in the detector. The Phase-I upgrade of the CMS HB and HE detectors aims to keep detector performance high by updating the photosensors and readout electronics rather than replacing the scintillator tiles themselves. The photosensors chosen for the upgraded system are silicon photomultipliers (SiPMs), and this will be the first large installation of SiPMs in a radiation environment. The installation of the upgraded HE system is planned for winter 2016–2017, whereas the HB system will be installed during the second long shutdown (LS2) of the LHC during 2019.

This paper discusses the upgrade of the HB and HE detectors with SiPMs, starting from a more in-depth discussion of the motivation for the Phase-I upgrade in section 2. This is followed by a description of the overall readout chain in section 3, a detailed discussion of the SiPMs with their control electronics in section 4, and a description of the front-end readout card in section 5. Full system test results are briefly reported in section 6 before finishing with a summary in section 7.

2 Motivation for the Phase-I upgrade

Radiation damage to the HCAL scintillator tiles is the main motivation for the Phase-I upgrade of the HB and HE detector readout. The full Phase-I upgrade was envisioned to be put in place during LS2, before the radiation damage became too large. However, the incurred radiation damage during the past running periods of the LHC has been higher than originally expected, resulting in an increased signal loss, in particular for the most forward regions. As a result, the decision was made to advance the HE upgrade schedule by 2 years. It is now understood [7] that the radiation damage does not only depend on the total ionizing dose (TID), but also on the dose rate, because of chemical effects related to oxygen diffusion. Higher dose rates result in less damage for the same TID. Since the dose rate during scintillator material testing was necessarily much higher than at the LHC, the incurred radiation damage to the detector has been larger than anticipated. The dependence of the response of the detector can be modelled by an exponential decay,

$$\text{response} \propto \exp\left(-\frac{\text{dose}}{D}\right), \tag{2.1}$$

where the decay constant D depends on the dose rate. Figure 1 shows the relative response of the HE scintillator during the LHC running periods in 2012, 2015, and 2016. The degradation over time is clearly visible, as is the change in slope when going to a higher instantaneous luminosity during 2016. More details on this measurement can be found in ref. [7].

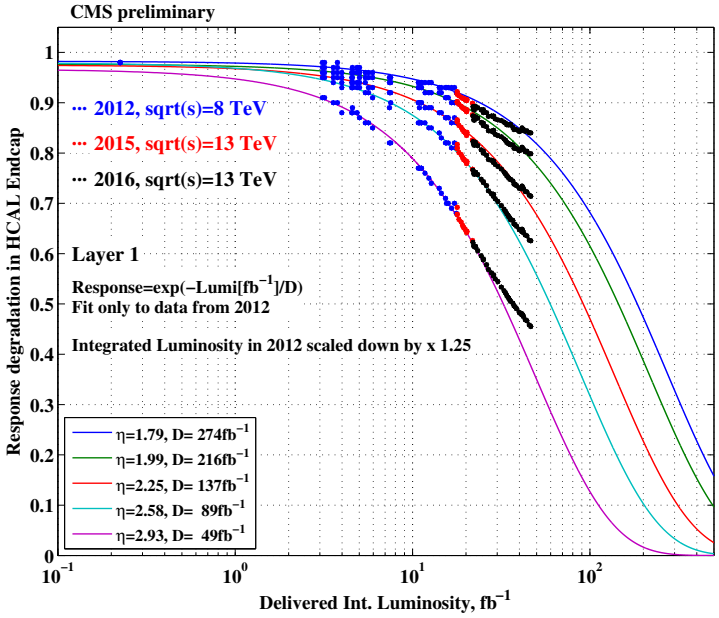

Figure 1. Response of the HE scintillator tiles as a function of the delivered integrated luminosity for several pseudorapidity values η. The blue, red, and black dots represent response measurements performed during 2012, 2015, and 2016, respectively. The integrated luminosity for 2012 has been scaled back to account for the different TID/fb^{-1} for 8 and 13 TeV collisions. The colored lines are fits to the 2012 measurements for different η values using the functional form from eq. (2.1). The box in the lower left corner contains the fitted value for the decay constant D for each fit.

The effect of this radiation damage on physics quantities, such as missing transverse energy and jet energy resolution, can be mitigated by replacing the HPDs with SiPMs. A key SiPM feature in this respect is the three times better photon detection efficiency compared to HPDs, which will directly increase the signal size. They are also much smaller, meaning that we can fit more channels in the same physical space. In the current system, the 17 detector layers are read out in 1–3 groups or 'depths', where the light from layers in any given group is optically added together by sending it to a single HPD. Therefore, having more channels allows for a finer depth segmentation, as shown in figure 2, which is ideal to perform a more precise calibration of the depth-dependent radiation damage. With the increased light yield and better calibration, the performance for physics quantities is recovered. For example, the upgrade results in an improvement of the jet energy resolution of >50% at $|\eta| \approx 2.8$–3 after 500 fb^{-1} of integrated luminosity is delivered by the LHC.

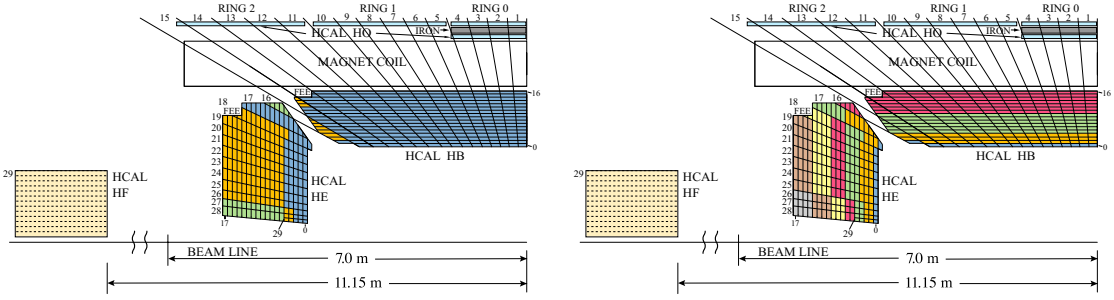

Figure 2. The HCAL depth segmentation in the current (left) and upgraded (right) system. Light from layers that are depicted with the same color are optically added together before reaching the photosensors.

3 The Phase-I readout chain

The upgraded HB and HE detectors consist of three main components: the active scintillator material, the on-detector or 'front-end' electronics, and the off-detector or 'back-end' electronics. The front-end electronics are organized into readout boxes, of which there are 36 for HE and 36 for HB. Each readout box contains four readout modules, a calibration unit, and a clock, control and monitoring unit (CCM). Each HE (HB) readout module consists of 48 (64) SiPMs in their thermal enclosure, an optical decoder unit (ODU) that maps the detector layers onto the SiPMs, a SiPM control card, and four front-end readout cards, as shown in figure 3. The calibration unit allows us to send LED light to the SiPMs, and the CCM handles the distribution of the clock and fast reset signals, as well as the control and monitoring of the front-end readout cards and SiPM control card.

The HE readout chain, shown schematically in figure 4, starts with the scintillation light from the active material that is wavelength-shifted and then sent to the SiPMs via clear optical fibers. The charge output from the SiPMs is then fed into the front-end readout cards, which each include twelve QIE11 ASICs [8] and one Microsemi Igloo2 FPGA. Each QIE11 integrates charge from one SiPM at 40 MHz without dead time. Each Igloo2 FPGA serializes and encodes the data from the twelve QIE11 channels. The encoded data is optically transmitted to the back-end electronics via the CERN Versatile Twin Transmitter (VTTx) [9] at 4.8 Gbps. The back-end electronics buffer the data, form trigger primitives, and ship the appropriate data to the central data-acquisition system

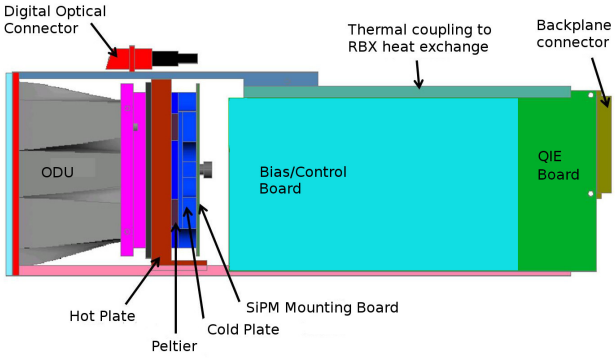

Figure 3. Illustration of the HE readout module, which consists of four front-end readout cards (or QIE boards), the optical decoder unit, the SiPMs in their thermal enclosure, and the SiPM control card.

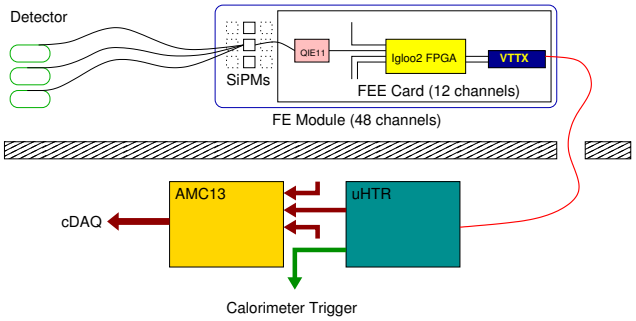

Figure 4. The data acquisition chain of the upgraded HE detector including the SiPMs, the front-end readout card and the optical link to the back-end electronics. The front-end readout card contains twelve QIE11 ASICs for charge integration, one Igloo2 FPGA for data serialization and encoding, and one VTTx optical transmitter.

upon receipt of a trigger accept signal. The HB readout chain is identical to the HE readout chain except for adjustments related to the increased channel count per front-end readout card.

4 Silicon photomultipliers and control electronics

The SiPMs used in the upgraded HE system have been produced by Hamamatsu. Two different SiPM sizes are used, 2.8 and 3.3 mm in diameter, in order to handle the varying number of scintillator layers that are optically added together. The SiPMs contain 4500 pixels/mm^2, each of which is operated in Geiger mode. The total SiPM signal is the sum of all fired pixels. The SiPMs have a fast recovery time of 10 ns, which increases the effective pixel count by a factor of about three by allowing each pixel to fire more than once during the illumination time of the scintillation light.

SiPMs have several advantages compared to the HPDs that are currently used in the CMS HCAL detector. SiPMs have a smaller size, a better photon detection efficiency of around 28–35%, and a very high gain ($2.7–3.5 \times 10^5$) that is two orders of magnitude larger than the HPD gain, assuming that the SiPMs are operated at 3–4 V above their breakdown voltage V_b. Figure 5 shows the SiPM photon detection efficiency and gain as a function of over-voltage $V - V_b$. In addition, the noise caused by spontaneous discharge of the high voltage through the HPD is eliminated for

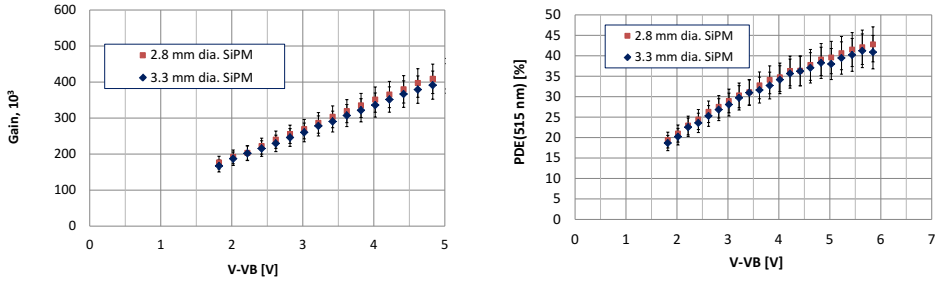

Figure 5. (Left) SiPM gain versus over-voltage for both SiPM sizes. (Right) Photon detection efficiency (PDE) for 515 nm light versus over-voltage for both SiPM sizes.

SiPMs because the SiPMs are not sensitive to magnetic fields and are operated at a much lower voltage of around 68 V compared to the roughly 8000 V that is needed for HPDs.

SiPMs also have several disadvantages compared to HPDs, in particular, the SiPM gain has a temperature dependence of 2%/°C and a voltage sensitivity of 30%/V. However, these temperature and voltage dependencies can be managed with careful detector design, as described below. The dark current is negligible for unirradiated SiPMs but reaches 50 μA at 3 V over-voltage and 5°C operation for a neutron fluence of $1 \times 10^{12}/\text{cm}^2$. Even with this level of dark current, SiPMs still possess better signal/noise than HPDs at high neutron fluence [10].

Eight SiPMs are mounted in a single package, and 6 of these packages are used per HE readout module. The packages are mounted on the SiPM mounting board, which is a rigid-flex construction with a rigid part that holds the SiPMs inside their cooling assembly, flex cables that interface with the QIE11 chips for the charge integration, and a flex cable that transfers the desired bias voltage to each SiPM independently. Temperature and humidity sensors are installed next to the SiPMs on the mounting board.

To achieve a SiPM gain stability and accuracy to within 1%, the SiPM control electronics must provide a precise control of the bias voltage and of the temperature. The SiPM control board generates the bias voltage (BV) needed to operate the SiPMs in two stages. In the first stage, a custom boost converter generates the bulk BV of $O(100\,\text{V})$ from the voltage on the backplane (about 9.5 V) of the readout box. This bulk BV is then stepped down to the operational voltage for each of the 48 individual SiPM channels. The value of the stepped-down voltage is tuneable from 0–80 V with 20 mV precision via a 12-bit DAC. For reference, the breakdown voltages of the SiPMs are around 65 V. This bias voltage tuning results in an approximate precision of 1% on the SiPM gain at an operating point of 3 V over the breakdown voltage.

The temperature of the SiPMs is controlled via a Peltier cooling element. The current temperature is read out from the sensor on the mounting board via the SiPM control board. An online software control loop configures the Peltier based on the difference between the measured value and the desired operating temperature of 5°C. A 12-bit DAC on the control board is used to tune the Peltier voltage, resulting in a temperature control precision of 0.01°C.

All 144 control boards needed for the HE installation have gone through quality control, and the response of each bias voltage channel has been measured. The channels are very uniform, with a response RMS of only 0.3%, and this small variation will be calibrated to achieve uniform SiPM gain across all channels of the detector.

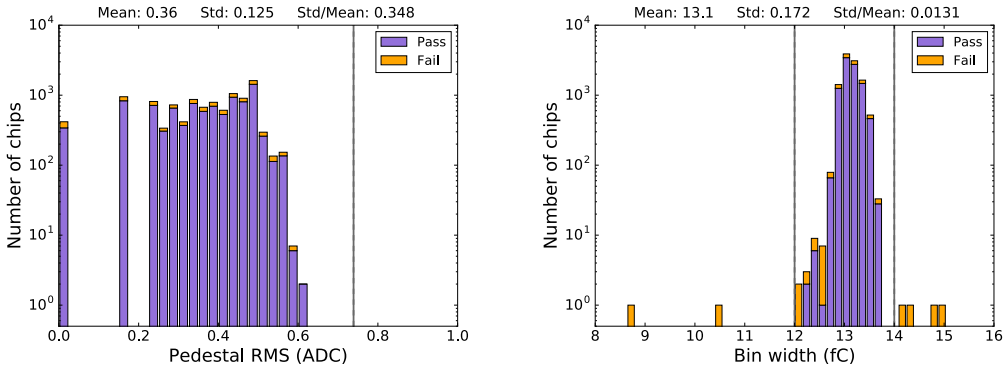

Figure 6. Two tests of the QIE11 ASIC with the corresponding selection criteria (grey vertical lines). The purple contribution corresponds to chips passing all selection criteria, while the orange indicates chips that failed at least one test. The y axis corresponds to the number of chips on a logarithmic scale. (Left) Measurement of the pedestal RMS in ADC counts. The mean pedestal RMS corresponds to ≈1.5 fC. (Right) Measurement of the bin width for the third subrange in the first range. For good chips, the mean bin width is 13.1 fC with a variation of about 1.3%.

5 Front-end readout card

The HE (HB) front-end readout card contains 12 (16) QIE11 ASICs, one (two) Microsemi Igloo2 FPGA, one VTTx module containing two 4.8 Gbps optical links, and one Microsemi ProASIC3L FPGA. The neccessary voltages for operating the front-end readout card are supplied by the radiation and magnetic field tolerant CERN FEASTMP DC-DC converters [11].

The Fermilab QIE11 ASIC integrates charge in 25 ns intervals and has a 17-bit dynamic range with 8-bit readout. The dynamic range is extended with respect to the previous generation (QIE8), which had a 14-bit dynamic range with 7-bit readout, in order to match the larger SiPM gain compared to HPDs. The QIE11 achieves a ≈1% resolution over the full dynamic range by using four integration ranges (scaled by factors of 8) with a 6-bit pseudo-logarithmic ADC, resulting in four subranges for each range. The dynamic range extends to 350 pC with the least significant bit corresponding to 3 fC. The QIE11 also features a programmable current shunt, with values that can range between 1 and 1/11.5, that makes it possible to tune the SiPM gain independently of the photon detection efficiency and increase the dynamic range even further.

All QIE11 chips are thoroughly tested after packaging, but before they are mounted on the front-end readout cards. A custom test setup is used, consisting of a test board and a robotic arm with vacuum head that moves the QIE chips. A total of 1120 chips can be loaded into the test setup. The test suite, which covers the full chip functionality, takes about 2.5 minutes per chip to complete. Very good acceptance was obtained, 98% for basic functionality checks, and 86% for the final selection which includes uniformity requirements. As an illustration, figure 6 shows the distribution of the QIE11 pedestal RMS and of the bin width of the third subrange in the first range. Chips that pass all selection requirements are shown in purple, whereas orange signifies chips that failed at least one component of the test suite.

The digitized data from all 12 (16) QIE11 chips on the HE (HB) front-end readout board is sent to the Igloo2 FPGA via an 8-bit 80 MHz bus using the LVDS standard. The Igloo2 FPGA is radiation

tolerant and is thus ideally suited for use in on-detector electronics receiving 10^{12} neutrons/cm^2, 10 krad of ionizing dose, and 10^{11} 20 MeV hadrons/cm^2 over 3000 fb^{-1}. It serializes the data and formats it using 8b/10b encoding. This encoded data is then sent via the VTTx to the μTCA-based back-end electronics [12]. The ProASIC3L FPGA is not a direct part of the data path. Rather, it is used as an I2C bridge between the CCM module on the one hand and the QIE11 and Igloo2 FPGA on the other hand. Any information regarding the configuration or current state of these chips passes through the ProASIC3L FPGA. It can also communicate with a temperature and humidity sensor on the front-end readout board, as well as the chip containing the board's unique identifier.

All HE front-end readout cards have gone through quality control in preparation of the upcoming installation. This includes a visual inspection upon arrival from the assembler and a range of tests such as reading and writing registers on the QIE11 ASICs and the FPGAs, checking the QIE11 pedestal values, and using the internal charge injection feature of the QIE11 ASIC to verify that the data is transmitted off the card in the correct way. A yield of 94% was obtained. Following the quality control, the response of each QIE11 ASIC on each readout card has been measured with negligible statistical uncertainty for all shunt values using a custom charge injector board, allowing the calibration of the initial 1.3% spread in the bin widths.

6 System testing

During the summer of 2015 the HE preproduction system was tested at the CERN H2 beamline using muon and pion beams of various energies. This test demonstrated the excellent performance of the SiPMs compared to the HPDs, especially in terms of signal-to-noise ratio. All features of the front-end readout cards were found to be fully functional and performing as expected. More details on this test can be found in ref. [13].

The upgraded HE front-end electronics were also subjected to radiation testing at the CHARM facility at CERN. Two one-week long tests were performed, in October 2015 for the preproduction system and in September 2016 for the final production system. The system was exposed to a total ionizing dose and 1 MeV-equivalent neutron fluence exceeding the levels expected to be accumulated during the lifetime of the HE system. No failures were observed during this time, and the measured rates of single event effects are manageable and within expectations.

7 Summary

The CMS experiment at the LHC is upgrading the endcap and barrel sections of its hadron calorimeter with silicon photomultipliers. About 16 000 readout channels will be present after the upgrade, making this the first large installation of SiPMs in a radiation environment. During the winter of 2016–2017, the endcap sections will be upgraded. The barrel sections will follow during the second long shutdown in 2019. The main motivation of the upgrade is to mitigate the effects of radiation damage to the scintillator tiles. This is done by replacing the existing hybrid photodiodes with new silicon photomultipliers which have a higher photon detection efficiency and much higher gain. To read out the data from the new photosensors, all associated front-end electronics will also be upgraded. The upgraded system will consist of readout modules housing the SiPMs, a calibration unit, and a clock, control and monitoring module. The readout modules also contain the SiPM

control electronics and the front-end readout cards, which feature the Fermilab QIE11 ASICs, the Microsemi Igloo2 FPGA, the CERN VTTx with two 4.8 Gbps optical links, and the Microsemi ProASIC3L FPGA. With these new electronics in place, the jet energy resolution will improve by >50% at $|\eta| \approx 2.8$–3 after 500 fb^{-1} of integrated luminosity is delivered by the LHC.

Acknowledgments

NS is supported by Fermi Research Alliance, LLC under Contract No. De-AC02-07CH11359 with the United States Department of Energy and by an Early Career Award (FNAL 14-05, PI J.Hirschauer) from the Department of Energy, Office of Science, Office of High Energy Physics.

References

[1] CMS Collaboration, *CMS Physics: Technical Design Report Volume 1: Detector Performance and Software*, CERN-LHCC-2006-001 (2006).

[2] Artur Lobanov for the CMS collaboration, *The CMS Outer HCAL SiPM Upgrade*, *J. Phys. Conf. Ser.* **587** (2015) 012005.

[3] Yasar Onel for the CMS collaboration, *CMS Hadron Forward Calorimeter Phase-I Upgrade Status*, *J. Phys. Conf. Ser.* **587** (2015) 012007.

[4] P.B. Cushman and A.H. Heering, *Problems and solutions in high-rate multi-channel hybrid photodiode design: the CMS experience*, *Trans. Nucl. Sci.* **49** (2002) 963.

[5] A. Baumbaugh, M. Binkley, X.Y. Chen, J.E. Elias, S. Hansen, S. Los, R. Tschirhart, T. Zimmerman and R.J. Yarema, *Charge integrator and encoder ASIC for readout of the CMS hadron calorimeter photodetectors*, Proceedings of *4th Workshop on Electronics for LHC experiments* (1998) p 250.

[6] CMS Collaboration, *The CMS experiment at the CERN LHC*, *JINST* **3** (2008) S08004.

[7] CMS Collaboration, *Dose rate effects in the radiation damage of the plastic scintillators of the CMS Hadron Endcap Calorimeter*, *JINST* **11** (2016) T10004.

[8] T. Roy, F. Yumiceva, J. Hirschauer, J. Freeman, E. Hughes, D. Hare, L. Dal Monte, A. Whitbeck and T. Zimmerman, *QIE: performance studies of the next generation charge integrator*, *JINST* **10** (2015) C02009.

[9] C. Soòs, M. Barros Marin, S. Détraz, L. Olanterä, C. Sigaud, S. Storey, J. Troska, F. Vasey and P. Vichoud, *The Versatile Transceiver: towards production readiness*, *JINST* **8** (2013) C03004.

[10] Yu. Musienko, A. Heering, R. Ruchti, M. Wayne, A. Karneyeu and V. Postoev, *Radiation damage studies of silicon photomultipliers for the CMS HCAL phase I upgrade*, *Nucl. Instrum. Meth. A* **787** (2015) 319.

[11] F. Faccio, G. Blanchot, C. Fuentes, S. Michelis, S. Orlandi, S. Saggini and I. Troyano, *FEAST2: A Radiation and Magnetic Field Tolerant Point-of-Load Buck DC/DC Converter*, IEEE Nucl. Sci. Symp. Conf. Rec. (2014).

[12] CMS Collaboration, *Technical proposal for the upgrade of the CMS detector through 2020*, CERN-LHCC-2011-006 (2011).

[13] N.J. Pastika on behalf of the CMS collaboration, *Performance of the prototype readout system for the CMS endcap hadron calorimeter upgrade*, *JINST* **11** (2016) C03020.